Comparison of transient grating signals from spheroidene in an organic solvent and in pigment-protein complexes from *Rhodobacter sphaeroides* 2.4.1

Mitsuru Sugisaki,[1,*] Masazumi Fujiwara,[1] Daisuke Kosumi,[1] Ritsuko Fujii,[1] Mamoru Nango,[1,2] Richard J. Cogdell,[3] and Hideki Hashimoto[1]

[1]*CREST-JST and Graduate School of Science, Osaka City University, 3-3-138 Sugimoto, Sumiyoshi, Osaka 558-8585, Japan*

[2]*CREST-JST and Graduate School of Engineering, Nagoya Institute of Technology, Gokiso, Showa, Nagoya 466-8555, Japan*

[3]*Division of Biochemistry and Molecular Biology, IBLS, University of Glasgow, Glasgow G12 8QQ, Scotland, United Kingdom*

(Received 28 December 2009; revised manuscript received 10 May 2010; published 11 June 2010)

The concurrent dynamics of the electronic excitation and vibronic oscillations of spheroidene have been investigated by means of the transient grating (TG) spectroscopy. The third-order optical responses of spheroidene in an organic solvent, in the LH2 light-harvesting antenna complexes, and in chromatophores have been compared in order to investigate the influence of the environment surrounding this photosynthetic pigment. Vibronic coherent oscillations with a period of several tens of femtosecond have been clearly observed superimposed on a slowly varying background, which reflects the electronic dynamics. The dynamics of the coherent oscillations have been analyzed by means of the wavelet analysis. Within our experimental accuracy, the decay times of the C=C and C—C stretching modes and C—CH_3 rocking mode of each specimen are very close. The experimental results have also been analyzed using a Brownian oscillator model. For these numerical calculations, the spectral density for the underdamped modes has been determined from the Raman spectrum of spheroidene. It was found that the low-frequency modes that reflect the influence of the protein environment can be approximated by the overdamped Brownian oscillator. The experimentally observed linear absorption spectra as well as the third-order optical responses, i.e., TG curves, are reproduced very well by these calculations. The close agreement between the experiments and calculations indicates that the Feynman-diagrammatic approach can be applied to express not only the internal conversion but also the intermolecular excitation energy-transfer processes. The vibronic decay rates of spheroidene in LH2 complexes and chromatophores are evaluated to be about 20% larger than in the organic solvent.

DOI: 10.1103/PhysRevB.81.245112 PACS number(s): 82.53.Kp, 42.65.Re, 63.22.−m, 78.20.Bh

I. INTRODUCTION

Carotenoids (Car) are one of the most abundant pigments found in nature and are known to play an important role of light harvesting in bacterial antenna complexes.[1,2] The primary processes of photosynthesis involve the capture of sunlight and efficient transfer of the resulting excitation energy to the reaction centers.[3] Carotenoids absorb photons in the blue green region of the spectrum. Since this spectral region corresponds to a gap between the absorption bands of (bacterio)chlorophylls, carotenoids act as accessory light-harvesting pigments.[1] This light-harvesting process involves singlet-singlet energy transfer from the donor carotenoids to the acceptor (bacterio)chlorophylls. The fluorescence-excitation measurements, together with time-resolved absorption spectroscopy, have revealed the highly efficient energy-transfer pathways from carotenoid to bacteriochlorophylls (BChl) in photosynthetic purple bacteria.[4–7] For example, almost 90% of the photons absorbed by the carotenoids are transferred to the BChl in the LH2 antenna complexes of *Rhodobacter* (*Rba.*) *sphaeroides* 2.4.1. Interestingly there is still considerable uncertainty as to the detailed mechanisms involved in these energy-transfer reactions.

When considering these excitation energy-transfer processes, it is necessary to determine the decay rates of the electronic excitations and the rates of the energy transfers taking place between the photosynthetic pigments.[2] It is also important to take the molecular vibrations into consideration since it is well known that the dynamics of electronic states is strongly influenced by those of the nuclei, as has been widely recognized in solid-state physics and physical chemistry in both exciton-phonon interactions and vibronic coupling.[8,9] For a unified understanding of the electronic and vibronic structures of photosynthetic pigments simultaneous observation of both their electronic and nuclear dynamics is necessary. According to the fluctuation-dissipation theorem since the spectral linewidth Γ of a Raman peak is related to the decay time T_2^* of the vibronic mode by $\Gamma=(\pi c T_2^*)^{-1}$, a Raman-scattering measurement should provide direct information on the dynamics of vibronic oscillations. Although Raman-scattering measurements of spheroidene have been reported,[10] most of them have mainly focused attention on the peak energies; this information is not enough to discuss the dynamics of the carotenoid's molecular vibrations. Furthermore, as reported by several authors, there are discrepancies between the decay rates evaluated by Raman measurements and those obtained by time domain measurements because of, for example, anharmonic interactions.[11,12] The results of x-ray crystallography on the antenna complexes from purple bacteria show that carotenoids bound to these light-harvesting proteins are rather twisted,[3,13] which may result in significant anharmonicity of their potential curves. Therefore, direct observation of the dynamics of their vibronic oscillations is required.

The ultrafast nonlinear responses of photosynthetic pigments have been described previously.[12,14–17] In these studies pump-probe and transient grating (TG) spectroscopies have

been widely used.[18] The most important advantage of the TG spectroscopy in comparison with the pump-probe technique is that the TG signal is background free since it is detected along the phase-matched direction of three pump pulses. Recently, the TG spectroscopy of carotenoids has been described.[12,14–16,19] In addition, Christensson *et al.*[20] have also reported the electronic structures of astaxanthin and lycopene using other third-order nonlinear spectroscopic techniques, i.e., three-pulse photon-echo and peak shifts. However, detailed TG signals from carotenoids bound in light-harvesting complexes have not been investigated previously.

In the present work, the vibronic coherent oscillations and the relaxation processes of electronic excitation of carotenoids in solvent and the peripheral light-harvesting antenna complexes LH2 from *Rba. sphaeroides* 2.4.1 have been compared by means of the TG spectroscopy. The advantage of using LH2 is that there is extensive information on its structure obtained by a combination of electron and atomic force microscopy.[21] Another important advantage of this system is that the electronic levels of pigments are spectrally well resolved, resulting in a clearly understandable absorption spectrum. The ultrafast spectroscopy on LH2 from *Rba. sphaeroides* has been performed by several groups, especially by means of the fluorescence up-conversion, two-photon excitation, and pump-probe techniques (see, for example, Refs. 2, 4–7, and 22–28). In this paper, ultrashort pulses of sub-20 fs duration have been used to examine the electronic and vibronic decay processes simultaneously.[29] The dynamics of the elementary excitations in spheroidene in and out of antenna proteins have been compared.

II. EXPERIMENTAL DETAILS

Chromatophores and LH2 complexes from *Rba. sphaeroides* 2.4.1 were prepared as previously described in Ref. 30. Spheroidene was isolated from the cells of *Rba. sphaeroides* 2.4.1 and then purified by twice recrystallizing from *n*-hexane.[31] For the optical measurements, the LH2 complexes and chromatophores were suspended in 20 mM Tris-HCl (pH 8.0) buffer and in the case of LH2 in the presence of 0.1% of LDAO (*N*,*N*-dimethyldodecylamine *N*-oxide). Spheroidene was dissolved in tetrahydrofuran (THF). Optical absorption spectra were recorded using a commercial spectrophotometer (JASCO, V-670).

A home-build noncollinear optical parametric amplifier (NOPA) pumped by a femtosecond Ti:sapphire regenerative amplifier (Spectra Physics, Hurricane) was used as the excitation light source for the TG measurements. Details of the NOPA together with the optical setup have been reported elsewhere.[14] For the TG spectroscopy, the compressed output beam from the NOPA was divided into three, using pellicle membranes with a thickness of 2 μm to avoid the additional frequency chirp. The temporal separation of each pulse was controlled using a translation stage that has an accuracy of better than 20 nm (which corresponds to a temporal step of 0.13 fs). The sample concentration was adjusted so that the optical density was between 0.2 and 1 at its absorption maximum. The pump pulses, in the triangular configuration, were focused onto the surface of a sample flow cell that has a thickness of 0.1 mm. After passing through the sample, the nonlinear signals were spatially selected using an iris of 1 mm diameter and then spectrally resolved using a 10 cm single monochromator (JASCO, HR10) equipped with a photomultiplier tube (Hamamatsu, R636-10). The signal was filtered and amplified by means of the lock-in technique. For the measurement of the Raman spectra, a cw diode-pumped solid-state laser at 532 nm was used for the excitation. The excitation power at the sample cell is set at 5 mW using a variable neutral density filter. The signal was resolved using a 30 cm single monochromator (Acton Research, SpectraPro 306i) and then detected by a liquid-nitrogen-cooled charge-coupled device camera (Roper Scientific, LN/CCD-1340/400-EB1). All the optical measurements were performed at room temperature.

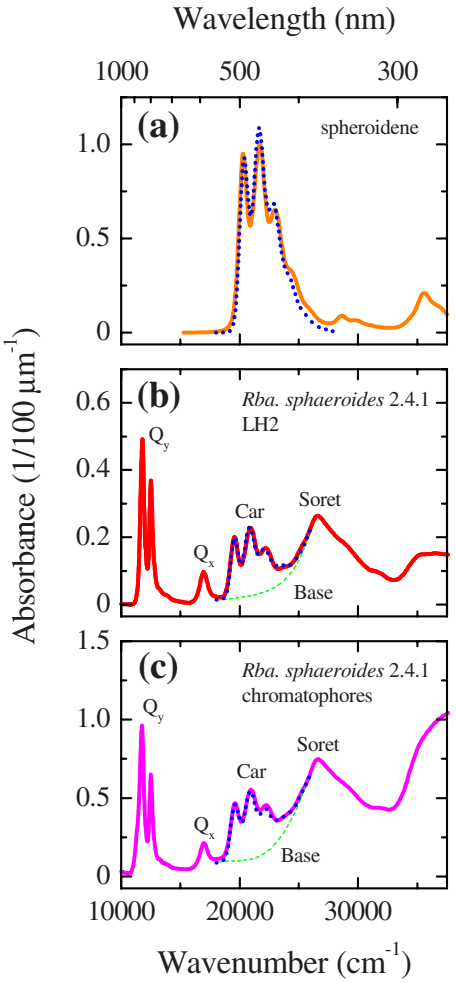

FIG. 1. (Color online) Absorption spectra of (a) spheroidene in THF, (b) LH2 complexes, and (c) chromatophores from *Rba. sphaeroides* 2.4.1. Solid curves: experimental results. Dotted curves: calculations. The absorption bands of carotenoids in Figs. 1(b) and 1(c) are denoted as "Car." The base levels shown by the dashed curves due to the Soret band of BChl were assumed.

III. RESULTS AND DISCUSSION

A. Stationary linear absorption spectra

The thick solid curves in Fig. 1 show the linear optical-

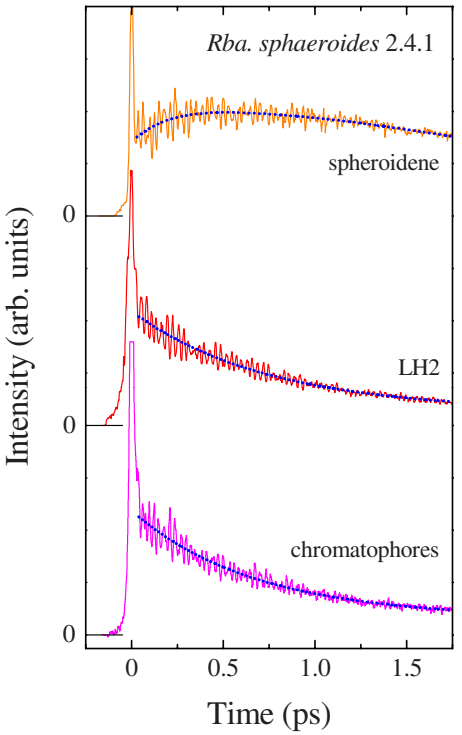

FIG. 2. (Color online) From top to bottom, TG signals from spheroidene in THF, LH2 complexes, and chromatophores. The abscissa shows the population period T. The temporal separation between pulses 1 and 2 (coherent period τ) was set to zero. The slowly varying background is shown by the dotted curve.

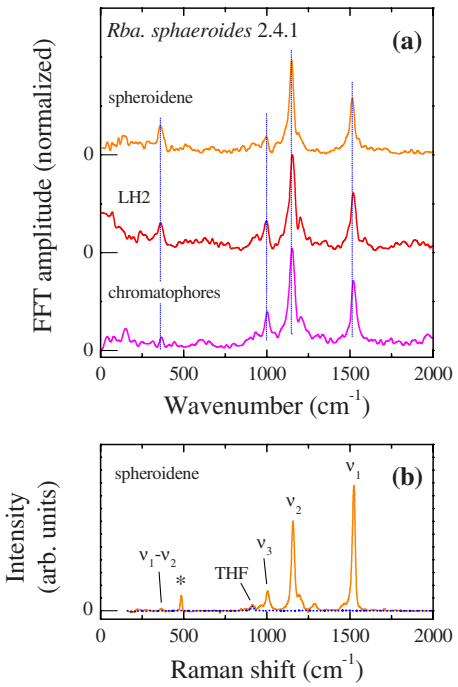

FIG. 3. (Color online) (a) FFT spectra of spheroidene in THF, LH2 complexes, and chromatophores obtained after the subtraction of the coherent spike and slowly varying background shown in Fig. 2. (b) Raman spectra of spheroidene (solid curve) and solvent THF (dotted curve). The coupled mode $\nu_1-\nu_2$ is observed at 364 cm^{-1}. The peak marked by the asterisk is an instrumental ghost line.

absorption spectra of (a) spheroidene, (b) LH2 complexes, and (c) chromatophores from *Rba. sphaeroides* 2.4.1. The pronounced structure with an absorption edge around 20 000 cm^{-1} is attributed to the optical transition from the $1\,^1A_g^-$ state (ground state, S_0) to the $1\,^1B_u^+$ state (excited state, S_2) of spheroidene, which is the main carotenoid found in *Rba. sphaeroides*. The absorption band is composed of several peaks with the energy spacing of ~1300 cm^{-1}, which indicates a strong coupling of the electronic state with the vibrational modes. In addition to the absorption band of Car, several other peaks are observed in Figs. 1(b) and 1(c). The absorption maxima observed at 27 000 and 17 000 cm^{-1} come from the Soret and Q_x bands of BChl, respectively. The Q_y band of BChl, with a doublet peak, is observed at 12 500 and 11 800 cm^{-1}. It is important to note that the absorption band of spheroidene is well resolved from that of BChl, i.e., the Q_x and Soret bands. This fact minimizes any ambiguities when determining the parameters of vibronic and electronic structures as discussed below.

B. Transient grating spectroscopy

From top to bottom, the solid curves in Fig. 2 show the TG signals from spheroidene in organic solvent and in LH2 complexes and chromatophores, where the temporal separation between pulses 1 and 2 (coherent period τ) was set to zero. The abscissa shows the temporal separation between pulses 2 and 3 (the population period T). The temporal widths of the pump pulses were optimized at 19 600 cm^{-1} for spheroidene in the organic solvent and 19 200 cm^{-1} for spheroidene in the LH2 complexes and chromatophores. Note that the spectral width of the excitation pulse was adjusted by placing a slit in the optical path of the pulse compressor of the NOPA so as not to excite the BChl Q_x band and spheroidene simultaneously.[16] Nonetheless the pulse width, determined by the cross correlation measurement, was better than 18 fs in all cases. In Fig. 2, an intense signal (coherent spike) was observed at $T=0$ of each TG curve. Coherent oscillations can be clearly seen with a period of about 20–30 fs that are superimposed on slowly varying components (dotted curves).

Each TG signal was analyzed by means of the fast Fourier-transform (FFT) technique as shown in Fig. 3(a). The coherent spike and slowly varying background are subtracted prior to the FFT to extract only the fast oscillating components. The Raman spectra of spheroidene (solid curve) and solvent THF (dotted curve) are also shown in Fig. 3(b) for comparison. The peak energies between the curves in Figs. 3(a) and 3(b) agree quite well to each other. It can, therefore, be concluded that the coherent oscillations observed in the TG curves come from the molecular vibronic oscillations of the ground state of spheroidene. The Raman peaks at $\nu_1=1522$ cm^{-1}, $\nu_2=1157$ cm^{-1}, and $\nu_3=1007$ cm^{-1} are assigned to be C═C symmetric stretching, C—C symmetric stretching, and the methyl-in-plane rocking mode, respectively.[32] These three dominant modes have been included in the following numerical calculations to evaluate the dynamics of the electrons and molecular vibra-

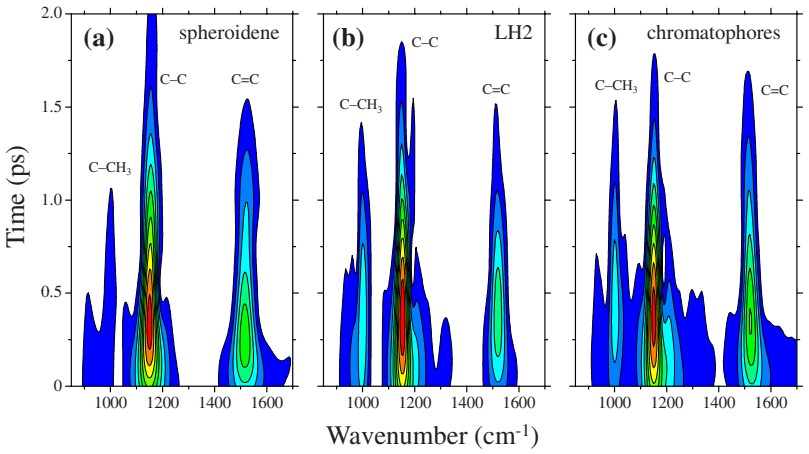

FIG. 4. (Color online) Temporal profiles of the vibronic oscillations of (a) spheroidene in THF, (b) LH2 complexes, and (c) chromatophores from *Rba. sphaeroides* 2.4.1 obtained by means of the wavelet analysis. Each spectrogram is normalized at the maximum of the C—C bond.

tions simultaneously. In addition to these modes a coupled mode $\nu_1 - \nu_2$ is also observed in the FFT spectra and is much clearer than that observed in the Raman spectrum. This result suggests a non-negligible effect of the anharmonicity of the potential curve especially in time-resolved measurements. A future theoretical study to determine more precise potential shapes compared to those calculated using the harmonic-oscillator model will be necessary.

The temporal profiles of the vibronic oscillations observed in the TG curves have been analyzed by means of a wavelet transformation technique. Since wavelets afford minimum Heisenberg uncertainty, they are especially useful for simultaneous time and frequency analysis of transient signals. The continuous wavelet transform of an analyzing signal $f(t)$ is defined as

$$F(a,b) = \frac{1}{\sqrt{a}} \int_{-\infty}^{\infty} f(t) \psi^* \left(\frac{t-b}{a} \right) dt. \quad (1)$$

The wavelet function $\psi(t)$ is characterized by a scale parameter a and a translation parameter b. In the present study, a complex Morlet (Gabor) wavelet has been used that is defined by

$$\psi(t) = \pi^{-1/4} \exp\left[i\omega_0 t - \frac{t^2}{2} \right]. \quad (2)$$

The advantage of the use of the Morlet wavelet is that its physical meanings are straightforward since it has a Gaussian window with the central frequency ω_0. In the present case, the wavenumber of the vibronic oscillations is characterized by the scale parameter a. The translation parameter b corresponds to the population period. Since both the temporal and spectral resolutions depend on the parameter ω_0, it is necessary to find the optimum value of ω_0 for the analysis. Here it was found that the decay times of the coherent oscillations are not influenced by the parameter ω_0 when ω_0 is higher than 8, which corresponds to the Gaussian width 350 fs at 1000 cm^{-1}. Therefore, in the following analysis, ω_0 was set to be 8 in order to obtain both the highest spectral and temporal resolutions.[12] All the peaks of the vibronic oscillations are clearly spectrally resolved under this condition, as shown below.

The contour plots in Fig. 4 show the temporal change in the amplitude of the coherent oscillations from spheroidene (a) in organic solvent, (b) in LH2 complexes, and (c) in chromatophores. Each spectrogram has been normalized at the maximum of the C—C bond vibration. One can clearly see the decay profiles of the vibronic oscillations. Further it was found that the peak energies of these vibrations shift with the change in the population period. This change is very slow (several 100 fs to 1 ps) compared to the period of the vibronic oscillations (a few tens of femtosecond). A time scale of 1 ps peak shift corresponds to a wavenumber of 30 cm^{-1}. We therefore consider that these shifts reflect the influence of low-frequency modes of the solvent and proteins surrounding spheroidene and the coupling is due to the anharmonicity of the potential curves.[33] A more detailed analysis of these shifts will be the subject of a future study but these data clearly illustrate that TG spectroscopy is a powerful technique and provides much more information than conventional Raman spectroscopy.

In order to evaluate the decay times of these oscillations, a single exponential decay function was used and fitted to the temporal profile of each vibrational mode to extract the most dominant decay constant. These calculated decay times of the coherent oscillations in the different samples are summarized in Fig. 5. The range of the error bars has been determined by careful repetition of the experiments (typically ten TG curves have been measured in each sample on different days). In each sample the decay times of the ν_1, ν_2, and ν_3 modes are very close.

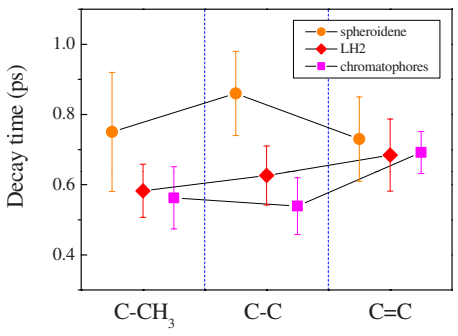

FIG. 5. (Color online) Decay times of the vibronic oscillations of spheroidene in THF (circles), LH2 complexes (diamonds), and chromatophores (squares).

In general, a proper evaluation of the decay times of both the vibronic oscillations and electronic excitation is in itself a difficult problem because the experimentally observed signal is a convolution of the electronic and vibronic decays. Namely, in a two-level system, the pure dephasing rate $1/T_2^*$ is evaluated from the relationship $1/T_2=1/2T_1+1/T_2^*$, where T_2 and T_1 are the total decay time of polarization and the lifetime of the excited state, respectively,[9,34] although the applicability of this phenomenological approach is still an open question.[35] Further, in the present case, since the electronic structures that we have to consider are different between the carotenoid in organic solvent and in the protein environment and have multiple levels (see Fig. 7), more detailed calculations are necessary to evaluate the dephasing time of the vibronic oscillations. Therefore the vibronic decay times have been evaluated using such a more rigorous model in the following sections.

C. Calculation of the steady-state absorption spectra

In order to analyze the experimental results, the Liouville space formalism was used to express the nonlinear response functions in terms of multitime correlation functions.[36] The numerical calculations were performed using the following procedures: (1) the spectral density $\rho(\omega)$ was modeled from the Raman spectrum that reflects the vibronic dynamics and the influence of the surrounding environment, followed by the conversion into a line broadening function $g(t)$,[37] (2) a set of the response functions representing all Liouville pathways was calculated by means of a second-order cumulant expansion, and then (3) the third-order nonlinear polarization was obtained by summing up the response functions. Based on the experimental data from the Raman spectrum, three Raman modes ν_1, ν_2, and ν_3 are introduced (see Fig. 3). The line shape of these modes was assumed, for simplicity, to be Lorentzian.[38] In order to take the influence of the surrounding proteins and solvent into account, an overdamped Brownian oscillator was introduced.[36] This model has been successfully used before to explain the TG signals from β-carotene and its homologs.[12,14–16] In this study, this model has been extended to spheroidene molecules bound to LH2 complexes and in chromatophores. The spectral density used for the calculation is shown in Fig. 6. It should be noted that several authors have reported low-frequency nuclear vibrations in the protein environments.[39] Since the reported spectra in the low-frequency region have complicated shapes, it is not clear what is the simplest and most appropriate function to statistically take account of the influence of the protein environment in the model. However, as shown below, it was found that an overdamped Brownian function that is represented by a single broad peak can reproduce well the linear and nonlinear optical responses.

The steady-state absorption spectra $\sigma_a(\omega)$ can be readily calculated using the line broadening function $g(t)$,[36]

$$\sigma_a(\omega) \propto \mathrm{Re}\int_0^\infty dt\, \exp[i(\omega-\omega_{eg})t-g(t)], \qquad (3)$$

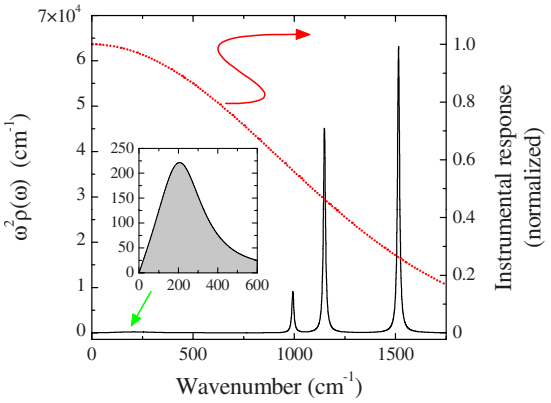

FIG. 6. (Color online) Solid curve: model spectral density of spheroidene in an organic solvent used for numerical calculations. Magnification of the overdamped mode that refracts the influence from environment is shown in inset. Dotted curve: the instrumental response of the pulse width of 18 fs.

where ω_{eg} indicates the energy separation between the S_0 and S_2 states. In the following numerical calculations, the cutoff frequency for the integration was set to 1700 cm^{-1} because the amplitude of $g(t)$ becomes very small above this frequency. The calculated spectra are shown by the thick dotted curves in Fig. 1. The parameters used in the calculation are summarized in Tables I and II. Since the absorption spectra of the carotenoid region of LH2 complexes and chromatophores are superimposed on the shoulder of the Soret band of BChl, we assumed, for the calculation, the baseline levels shown by the thin dashed curves in Figs. 1(b) and 1(c). It was found that good agreement between the experimental results and numerical calculations could be obtained in all cases.

D. Calculation of the TG signals

As the first step of the calculation of the TG curves, we must determine the electronic and vibronic parameters of spheroidene in the solvent. The TG signals were calculated under conditions of the impulsive limit. The energy diagram shown in Fig. 7(a) was assumed: the ground state S_0, the first low-lying excited singlet state S_1 that is one photon forbidden, and the lowest, one photon allowed singlet state S_2. Furthermore, an intermediate state, S_x, between S_1 and S_2 has been introduced in our calculations. As reported in Ref. 16, the intermediate state S_x is necessary to reproduce the

TABLE I. Common parameters used for the numerical calculations. Δ_{in}: inhomogeneous broadening, ω_B: frequency of Brownian oscillator, γ_B: damping constant, and μ_{ij}: transition dipole interaction between S_i and S_j.

Δ_{in} (cm^{-1})	0
ω_B (cm^{-1})	250
γ_B (cm^{-1})	300
μ_{T2}/μ_{20}	0.3
$\mu_{\xi x}/\mu_{20}$	0.7

TABLE II. Intrinsic parameters of spheroidene in solvent, LH2 complexes, and chromatophores. ω_{eg}: thermally averaged electronic energy gap, Γ: homogeneous linewidth, and λ_B: reorganization energy.

	Spheroidene	LH2	Chromatophores
ω_{eg} (cm^{-1})	22100	21350	21400
Γ (cm^{-1})	12	15	15
λ_B (cm^{-1})	380	300	380

spectral dependence of the TG curves of carotenoids (especially the rise of the signal observed around $T<200$ fs).[40] In addition to these states, it is very important to include the higher excited states S_T and S_ξ that are accessible through the two-step absorption processes (the so-called excited-state absorption).[12,14–16] In the present case, the first step absorption process is S_0 to S_2, where the population in S_2 is formed by the first and second pulses in the TG pulse sequence. The S_T state is accessible from the S_2 state. However, as has already been discussed in Ref. 16 since the internal conversion from S_2 to S_x is very fast most of the population relaxes into the S_x state before it is excited into the S_T state. The second step absorption process from S_x to S_ξ takes place as a result of irradiation by the third pulse.

As shown in Fig. 7(a), the successive cascade process from S_2 to S_0 via S_x and S_1 is considered for simplicity. Since the direct population decay rate from S_2 to S_0 is much smaller than that from S_2 to S_x, this assumption is appropriate and significantly simplifies the calculation, resulting in a reduction in the required total numerical computation time. The rate equations of the population kinetics can be represented as

$$\frac{dn_2}{dt} = -\Gamma_{2x} n_2,$$

$$\frac{dn_x}{dt} = \Gamma_{2x} n_2 - \Gamma_{x1} n_x,$$

$$\frac{dn_1}{dt} = \Gamma_{x1} n_x - \Gamma_{10} n_1,$$

$$\frac{dn_0}{dt} = \Gamma_{10} n_1, \tag{4}$$

where n_i and Γ_{ij} indicate the population of the S_i, state and the internal-conversion rate between the S_i, and S_j, states, respectively. According to this population kinetics, each response function is separated into the nuclear and electronic population dynamic terms.[42] In other words, the experimentally observed decay profile with vibronic oscillations is a convolution of the pure dephasing and electronic decay.

In the present calculation with spheroidene in THF, the diagrams shown in Fig. 5 in Ref. 16 have been used. In the following calculations the same line broadening functions for the excited states as with the ground state were employed for simplicity. The process R_3 has not been included in the calculation because the direct relaxation from S_2 to S_0 can be assumed to be negligibly small as mentioned above. In addition, since the contribution of the excited-state absorption process from the S_1 state is small in the spectral region used in the present study, the process R_{6x} has also been omitted.

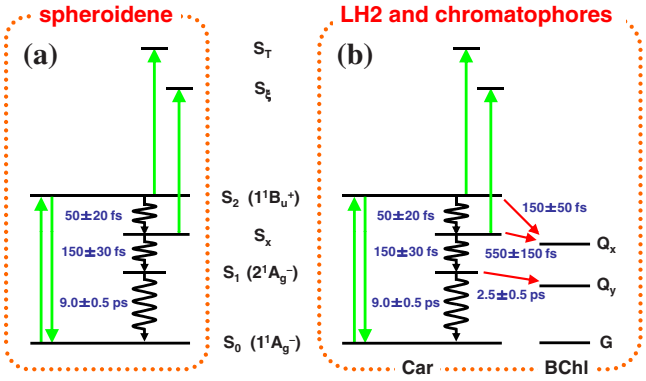

FIG. 7. (Color online) Energy diagrams of Car and BChl. The vertical arrows represent the optical pumping and dumping while the wavy lines show the internal conversion. The arrows pointing from Car to BChl levels indicate the excitation energy-transfer pathways.

The thin curve in Fig. 8(a) shows the TG signal calculated using the same set of parameters as those used for the calculation of the absorption spectrum (Tables I and II). The internal-conversion rates are shown in Fig. 7(a). Since the decay time of each vibronic mode of spheroidene in THF are very close, within the experimental error as shown in Fig. 5, a single value has been employed for the linewidth of the vibronic mode, i.e., 12 cm^{-1},[43] which corresponds to a dephasing time of 0.88 ps. Both the fast coherent oscillations and slowly varying background observed in the experiment are well reproduced. This result indicates that both the internal-conversion rates and the spectral density, including the vibronic decay rate employed in the present study, are appropriate for calculating both the linear and nonlinear optical responses. The signals near the origin of the time axis have not been shown because the calculation was performed in the impulsive limit and it is difficult in principle to reproduce the coherent artifact. The internal-conversion processes of spheroidene have been investigated by several groups. Within experimental error, the lifetime of S_1 obtained here agrees with that obtained by other spectroscopies, such as transient absorption[5–7,26–28,44] and two-photon excitation techniques.[24] The transient absorption and fluorescence upconversion techniques may, in principle, access the S_2 and S_x states but most of the previous studies have only included the S_2 state in their analyses. Therefore, it is hard to discuss the consistency between the present and previous studies. Nonetheless if we set the time constant of the S_x to S_1 process, i.e., 150 ± 30 fs, this actually corresponds well with the values reported as the S_2 lifetime in the previous papers.[6,22]

Now the TG signal from the LH2 complexes and chromatophores are analyzed. In these cases, the excitation energy-transfer pathways from spheroidene to BChl have to be taken into consideration. The rate equations based on the model schematically shown in Fig. 7(b) can be represented as

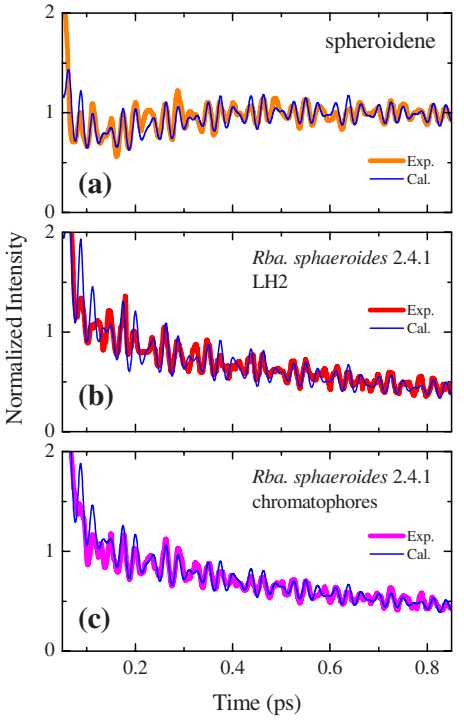

FIG. 8. (Color online) Comparison of the TG signals. Thin curve: experimental result. Thick curve: calculation.

$$\frac{dn_2}{dt} = -(\Gamma_{2x} + \Gamma_{2Q_x})n_2,$$

$$\frac{dn_x}{dt} = \Gamma_{2x}n_2 - (\Gamma_{x1} + \Gamma_{xQ_x})n_x,$$

$$\frac{dn_1}{dt} = \Gamma_{x1}n_x - (\Gamma_{10} + \Gamma_{1Q_y})n_1,$$

$$\frac{dn_0}{dt} = \Gamma_{2Q_x}n_2 + \Gamma_{xQ_x}n_x + (\Gamma_{1Q_y} + \Gamma_{10})n_1, \quad (5)$$

where the transfer rates of the electronic excitations from the S_2 and S_x states of carotenoid to the Q_x state of BChl are given by Γ_{2Q_x} and Γ_{xQ_x}, respectively. The electronic structure and the internal-conversion rate of carotenoid in the protein are assumed to be the same as the free carotenoid; the parameters for the excitation energy transfer are simply then included. The transfer rate from S_1 to Q_y is represented by Γ_{1Q_y}. In the present model, it was assumed that spheroidene returns to the ground state after the electronic excitation (population) is transferred to BChl. By considering all these states appropriately, it is possible to reproduce the TG signals measured in our experiments.

Based on this model, the Feynman diagrams used for the calculation of the TG signals of spheroidene in the LH2 complexes and chromatophores are described as shown in Fig. 9. The symbols i (i=0, 1, 2, x, T, and ξ) in the diagrams indicate the S_i state of carotenoid. The diagrams for the response functions R_1 and R_2 are the same as those used for a two-level system. The process R_4 includes the excited-state absorption into the S_T state from S_2. The other processes include the internal conversions that are represented by the vertically aligned dots. For example, in process R_{5x}, the population is formed by the first and second pump pulses in S_2 and then the population decays into S_0 via S_x and S_1, before the third pump pulse arrives. The symbols in the dotted boxes represent the excitation energy-transfer processes from carotenoid to BChl. For example, in process R_{4Q} the population formed in S_2 decays into S_x and is followed by energy transfer into the Q_x band of BChl. In this case the carotenoid returns to the ground state S_0. It should be emphasized that not only the internal-conversion processes but also the excitation energy transfer between molecules can be expressed by the Feynman diagrams, which enable us to compute the response functions in Liouville space.[36,45]

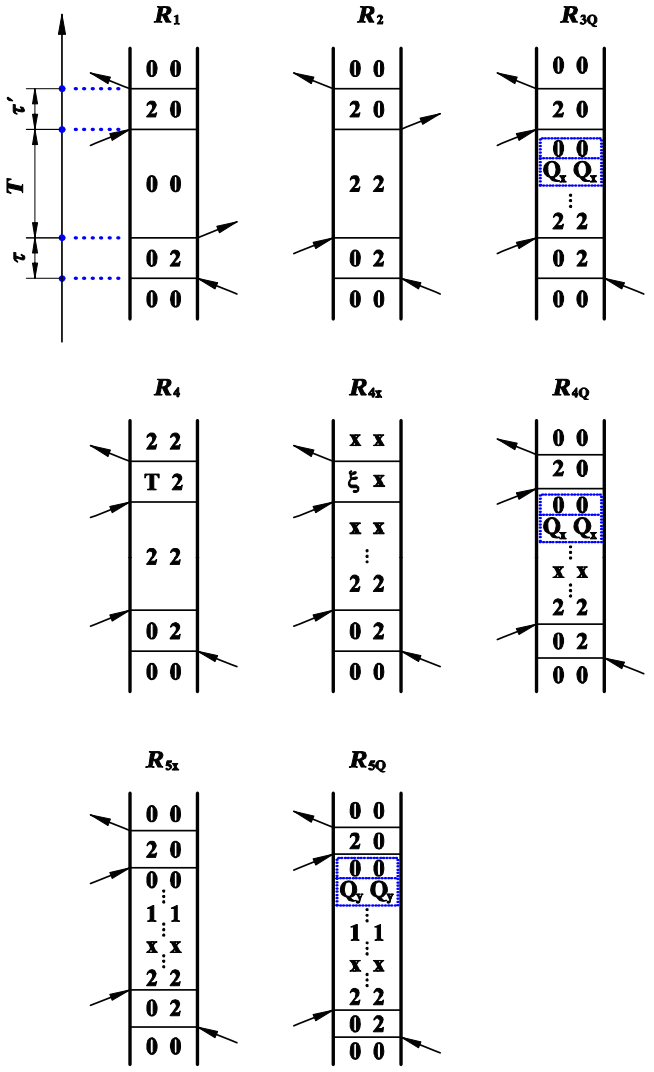

FIG. 9. (Color online) Double-sided Feynman diagrams based on the energy diagram shown in Fig. 7(b). The symbols in the dotted boxes represent the excitation energy-transfer processes from carotenoid to BChl.

The thin solid curves in Figs. 8(b) and 8(c) show the calculated TG signals from spheroidene in the LH2 complexes and chromatophores. Again the experimental results

are reproduced quite well. It should be noted that the internal-conversion rates of spheroidene bound to the proteins are assumed to be the same as for the free carotenoid (see Fig. 7). Within our experimental accuracy a difference in the internal-conversion rates of carotenoids between the organic solvent and proteins was not detected.[46] The linewidths used for the calculation 15 cm^{-1}, which corresponds to the vibronic decay of 0.71 ps and is faster by about 20% than that of spheroidene in the organic solvent.[47] As mentioned above, since most of the previous studies do not include the S_x state, it is hard to discuss the exact rates of the excitation energy transfer. However if we focus on the fastest pathway in the present study, i.e., 150 ± 50 fs of S_2 to Q_x, this agrees well with the results obtained in the previous studies.[5,6,22] The rate of S_1 to Q_y also agrees with those measured by some workers using other spectroscopic techniques within the limits of our experimental error[7,24,27] but is slightly slower in comparison with several other reports.[5,6,26] Nonetheless the rather good agreement between all the experimental data and calculation supports the validity of our model and the appropriateness of the values of the parameters used in these calculations. We consider the possible slow rate of S_1 to Q_y evaluated here may probably be because of our limited temporal range of T where the experiential accuracy of the slow decay times is about ± 0.5 ps (see Fig. 7).

Finally we briefly discuss the efficiency of the excitation energy transfer from carotenoid to BChl in LH2 complexes. The efficiency differs among species, for example, that of *Rba. sphaeroides* G1C or *Rba. sphaeroides* 2.4.1 is about 90% while those of *Rsp. molischianum* and *Rps. acidophila* 10 050 are about 50%.[4–6,25,48] This difference is explained by the number of the energy-transfer channels in operation in the different cases. Namely, when the number of conjugation double bonds of the carotenoid is $n \geq 11$, only excitation energy transfer from S_2 to Q_x takes place and the transfer rate from S_1 to Q_y becomes very low, resulting in an overall low efficiency. When $n \leq 10$, however, the $S_1 \rightarrow Q_y$ channel opens and the overall energy-transfer efficiency is increased by about 40%. The total efficiency obtained from our experimental results is 87%, which is in good agreement with previous studies using by the absorption and fluorescence-excitation measurements.[4–6,25] However the efficiency from S_1 to Q_y in our present study is 46%, which is higher than the previous reports,[5] namely, 21%. At this time it is difficult to discuss the significance of this difference because the branching ratios among the pathways are simply obtained from the time constants and depend strongly on the model employed.[4–6] Namely, if one of the electronic levels is missing or the time constants contain an error, the efficiency may change a little.[49] Therefore, for more precise evaluation, the measurements over wider spectral and temporal ranges are necessary to minimize the error bars.

IV. SUMMARY

We have investigated the dynamics of the electronic excitation and vibronic oscillations of spheroidene of three environmental conditions, an organic solvent THF, the LH2 antenna complexes, and chromatophores from *Rba. sphaeroides* 2.4.1. Coherent vibronic oscillations having a period of a few tens of femtosecond were clearly observed by means of the TG spectroscopy. By comparing the FFT spectra of the TG signals and Raman spectrum of spheroidene, it can be concluded that the vibronic oscillations mainly come from the C—C and C=C stretching modes and C—CH_3 in-plane rocking mode in the ground state. The wavelet analysis of the TG curves shows that the difference of the decay times of these vibronic modes is small in each sample. In addition to the dynamics of the vibronic oscillations, the pathways of the electronic excitation have been also investigated that is observed as the slowly varying background in the TG signals. The experimental results have been compared with the numerical calculations that are based on the Brownian oscillator model. The electronic structure of carotenoid and the internal-conversion rates used for the calculations are the same both in solvent and in the proteins. It was found that an overdamped Brownian function can approximate quite well the influence of the protein environment surrounding pigments on their liner and nonlinear optical responses. The excitation energy-transfer processes as well as the internal conversion are modeled within the framework of Lioville space pathways. The experimentally observed linear absorption spectra and nonlinear TG signals were reproduced well by our calculations, suggesting that the present model is valid. It is found that the decoherence of the vibronic oscillations in free solvent is about 20% slower than those in spheroidene in the LH2 complexes and chromatophores.

In addition to the TG experiment, the present paper reports a general framework to use the Feynman-diagrammatic approach that can be readily extended for including some additional electronic states. Since the branching ratio of the excitation energy transfer is simply evaluated by the rise and decay constants of each electronic state, the TG spectroscopy over a wide spectral range is necessary to take other electronic states precisely into consideration while further instrumental development is required. This is left for a subject for the future study.

ACKNOWLEDGMENTS

This work was supported in part by the Grant-in-aid from the Japanese Ministry of Education, Culture, Sports, Science, and Technology (Grants No. 18340091 and No. 22340085). R.J.C. acknowledges funding by the BBSRC. H.H. thanks Nissan Science Foundation and HFSP for financial support.

*Corresponding author; mitsuru@sci.osaka-cu.ac.jp

[1] H. A. Frank and R. J. Cogdell, Photochem. Photobiol. **63**, 257 (1996).

[2] As review articles, T. Polívka and V. Sundström, Chem. Rev. **104**, 2021 (2004); Chem. Phys. Lett. **477**, 1 (2009).

[3] H. van Amerongen, L. Valkunas, and R. van Grondelle, *Photosynthetic Excitons* (World Scientific, Singapore, New Jersey, London, Hong Kong, 2000); R. E. Blankenship, *Molecular Mechanisms of Photosynthesis* (Blackwell Science, Oxford, 2002).

[4] E. Papagiannakis, J. T. M. Kennis, I. H. M. van Stokkum, R. J. Cogdell, and R. vanGrondelle, Proc. Natl. Acad. Sci. U.S.A. **99**, 6017 (2002).

[5] Y. Koyama, F. S. Rondonuwu, R. Fujii, and Y. Watanabe, Biopolymers **74**, 2 (2004); F. S. Rondonuwu, K. Yokoyama, R. Fujii, Y. Koyama, R. J. Cogdell, and Y. Watanabe, Chem. Phys. Lett. **390**, 314 (2004).

[6] H. Cong, D. M. Niedzwiedzki, G. N. Gibson, A. M. LaFountain, R. M. Kelsh, A. T. Gardiner, R. J. Cogdell, and H. A. Frank, J. Phys. Chem. B **112**, 10689 (2008).

[7] J. P. Zhang, R. Fujii, P. Qian, T. Inaba, T. Mizoguchi, Y. Koyama, K. Onaka, Y. Watanabe, and H. Nagae, J. Phys. Chem. B **104**, 3683 (2000).

[8] E. I. Rashba and M. D. Sturge, *Excitons* (North-Holland, Amsterdam, 1982); M. Ueta, H. Kanzaki, K. Kobayashi, Y. Toyozawa, and E. Hanamura, *Excitonic Processes in Solids* (Springer-Verlag, Berlin, New York, 1982).

[9] W. W. Parson, *Modern Optical Spectroscopy: With Examples from Biophysics and Biochemistry* (Springer-Verlag, Berlin, 2006).

[10] See, for example, M. Lutz, I. Agalidis, G. Hervo, R. J. Cogdell, and F. Reisshusson, Biochim. Biophys. Acta **503**, 287 (1978); Y. Koyama, M. Kito, T. Takii, K. Saiki, K. Tsukida, and J. Yamashita, *ibid.* **680**, 109 (1982); M. Lutz, W. Szponarski, G. Berger, B. Robert, and J. M. Neumann, *ibid.* **894**, 423 (1987); P. Kok, J. Köhler, E. J. J. Groenen, R. Gebhard, I. van der Hoef, J. Lugtenburg, A. J. Hoff, R. Farhoosh, and H. A. Frank, *ibid.* **1185**, 188 (1994); N. Ohashi, N. KoChi, M. Kuki, T. Shimamura, R. J. Cogdell, and Y. Koyama, Biospectroscopy **2**, 59 (1996); P. Kok, J. Köhler, E. J. J. Groenen, R. Gebhard, I. van der Hoef, J. Lugtenburg, R. Farhoosh, and H. A. Frank, Spectrochim. Acta, Part A **53**, 381 (1997); R. Fujii, C. H. Chen, T. Mizoguchi, and Y. Koyama, *ibid.* **54**, 727 (1998).

[11] J. Menéndez and M. Cardona, Phys. Rev. B **29**, 2051 (1984); M. Hase, K. Mizoguchi, H. Harima, S. Nakashima, and K. Sakai, *ibid.* **58**, 5448 (1998).

[12] M. Fujiwara, K. Yamauchi, M. Sugisaki, A. Gall, B. Robert, R. J. Cogdell, and H. Hashimoto, Phys. Rev. B **77**, 205118 (2008).

[13] G. McDermott, S. M. Prince, A. A. Freer, A. M. Hawthornthwaite-Lawless, M. Z. Papiz, R. J. Cogdell, and N. W. Isaacs, Nature (London) **374**, 517 (1995); R. J. Cogdell, N. W. Isaacs, T. D. Howard, K. McLuskey, N. J. Fraser, and S. M. Prince, J. Bacteriol. **181**, 3869 (1999); K. McLuskey, S. M. Prince, R. J. Cogdell, and N. W. Isaacs, Biochemistry **40**, 8783 (2001).

[14] M. Sugisaki, K. Yanagi, R. J. Cogdell, and H. Hashimoto, Phys. Rev. B **75**, 155110 (2007).

[15] M. Sugisaki, M. Fujiwara, K. Yanagi, R. J. Cogdell, and H. Hashimoto, Photosynth. Res. **95**, 299 (2008).

[16] M. Sugisaki, M. Fujiwara, S. V. Nair, H. E. Ruda, R. J. Cogdell, and H. Hashimoto, Phys. Rev. B **80**, 035118 (2009).

[17] M. Sugisaki, R. Fujii, R. J. Cogdell, and H. Hashimoto, Photosynth. Res. **95**, 309 (2008).

[18] See also, G. Cerullo, D. Polli, G. Lanzani, S. De Silvestri, H. Hashimoto, and R. J. Cogdell, Science **298**, 2395 (2002); D. Polli, G. Cerullo, G. Lanzani, S. De Silvestri, K. Yanagi, H. Hashimoto, and R. J. Cogdell, Phys. Rev. Lett. **93**, 163002 (2004); H. Hashimoto, K. Yanagi, M. Yoshizawa, D. Polli, G. Cerullo, G. Lanzani, S. De Silvestri, A. T. Gardiner, and R. J. Cogdell, Arch. Biochem. Biophys. **430**, 61 (2004); D. Kosumi, M. Fujiwara, R. Fujii, R. J. Cogdell, H. Hashimoto, and M. Yoshizawa, J. Chem. Phys. **130**, 214506 (2009), and references therein.

[19] T. Hornung, H. Skenderovic, and M. Motzkus, Chem. Phys. Lett. **402**, 283 (2005); J. Hauer, H. Skenderovic, K. L. Kompa, and M. Motzkus, *ibid.* **421**, 523 (2006); J. Hauer, T. Buckup, and M. Motzkus, J. Phys. Chem. A **111**, 10517 (2007); Chem. Phys. **350**, 220 (2008); T. Buckup, J. Hauer, J. Mohring, and M. Motzkus, Arch. Biochem. Biophys. **483**, 219 (2009).

[20] N. Christensson, T. Polivka, A. Yartsev, and T. Pullerits, Phys. Rev. B **79**, 245118 (2009).

[21] See, for example, T. Walz, S. J. Jamieson, C. M. Bowers, P. A. Bullough, and C. N. Hunter, J. Mol. Biol. **282**, 833 (1998); S. Scheuring, J. Seguin, S. Marco, D. Levy, C. Breyton, B. Robert, and J. L. Rigaud, *ibid.* **325**, 569 (2003); S. Bahatyrova, R. N. Frese, C. A. Siebert, J. D. Olsen, K. O. van der Werf, R. van Grondelle, R. A. Niederman, P. A. Bullough, C. Otto, and C. N. Hunter, Nature (London) **430**, 1058 (2004); S. Scheuring, D. Levy, and J. L. Rigaud, Biochim. Biophys. Acta **1712**, 109 (2005); S. Scheuring, T. Boudier, and J. N. Sturgis, J. Struct. Biol. **159**, 268 (2007); L. N. Liu, T. J. Aartsma, and R. N. Frese, FEBS J. **275**, 3157 (2008); J. N. Sturgis and R. A. Niederman, Photosynth. Res. **95**, 269 (2008).

[22] M. Ricci, S. E. Bradforth, R. Jimenez, and G. R. Fleming, Chem. Phys. Lett. **259**, 381 (1996).

[23] T. H. Joo, Y. W. Jia, J. Y. Yu, D. M. Jonas, and G. R. Fleming, J. Phys. Chem. **100**, 2399 (1996); R. Z. B. Desamero, V. Chynwat, I. van der Hoef, F. J. Jansen, J. Lugtenburg, D. Gosztola, M. R. Wasielewski, A. Cua, D. F. Bocian, and H. A. Frank, J. Phys. Chem. B **102**, 8151 (1998); R. Jimenez, F. van Mourik, J. Y. Yu, and G. R. Fleming, *ibid.* **101**, 7350 (1997); K. Timpmann, N. W. Woodbury, and A. Freiberg, *ibid.* **104**, 9769 (2000); E. Papagiannakis, I. H. M. van Stokkum, M. Vengris, R. J. Cogdell, R. van Grondelle, and D. S. Larsen, *ibid.* **110**, 5727 (2006).

[24] P. J. Walla, P. A. Linden, C. P. Hsu, G. D. Scholes, and G. R. Fleming, Proc. Natl. Acad. Sci. U.S.A. **97**, 10808 (2000).

[25] H. Hörvin Billsten, J. L. Herek, G. Garcia-Asua, L. Hashoj, T. Polívka, C. N. Hunter, and V. Sundström, Biochemistry **41**, 4127 (2002).

[26] T. Polívka, T. Pullerits, H. A. Frank, R. J. Cogdell, and V. Sundström, J. Phys. Chem. B **108**, 15398 (2004).

[27] T. Polívka, D. Niedzwiedzki, M. Fuciman, V. Sundström, and H. A. Frank, J. Phys. Chem. B **111**, 7422 (2007).

[28] T. Polívka, D. Zigmantas, J. L. Herek, Z. He, T. Pascher, T. Pullerits, R. J. Cogdell, H. A. Frank, and V. Sundström, J. Phys. Chem. B **106**, 11016 (2002).

[29] Preliminary results of this study have been reported at M. Sugisaki, M. Fujiwara, R. Fujii, K. Nakagawa, M. Nango, R. J. Cogdell, and H. Hashimoto, International Conference on Luminescence and Optical Spectroscopy of Condensed Matter

(ICL'08), 2008 J. Lumin. **129**, 1908 (2009).

[30] R. J. Cogdell, I. Durant, J. Valentine, J. G. Lindsay, and K. Schmidt, Biochim. Biophys. Acta **722**, 427 (1983); M. B. Evans, R. J. Cogdell, and G. Britton, *ibid.* **935**, 292 (1988).

[31] R. Fujii, K. Onaka, M. Kuki, Y. Koyama, and Y. Watanabe, Chem. Phys. Lett. **288**, 847 (1998).

[32] S. Saito and M. Tasumi, J. Raman Spectrosc. **14**, 310 (1983); S. Saito, M. Tasumi, and C. H. Eugster, *ibid.* **14**, 299 (1983); A. M. Dokter, M. C. van Hemert, C. M. In 't Velt, K. van der Hoef, J. Lugtenburg, H. A. Frank, and E. J. J. Groenen, J. Phys. Chem. A **106**, 9463 (2002); S. Schlücker, A. Szeghalmi, M. Schmitt, J. Popp, and W. Kiefer, J. Raman Spectrosc. **34**, 413 (2003).

[33] The interference between the coherent oscillations in the excited and ground states can also cause the spectral shift. In the present case, the decay from S_2 to S_x is very fast as shown in Fig. 7 that corresponds to a few oscillation periods. Further since this is a stochastic process the memory of the coherent oscillations in the excited state is lost in this internal-conversion process. Therefore the coherent coupling between the oscillations in the excited and ground states is less plausible in the present case since the observed spectral shift is a picosecond range.

[34] A. Laubereau and W. Kaiser, Rev. Mod. Phys. **50**, 607 (1978); P. Schellenberg, R. J. W. Louwe, S. Shochat, P. Gast, and T. J. Aartsma, J. Phys. Chem. B **101**, 6786 (1997).

[35] A. Ishizaki and Y. Tanimura, J. Chem. Phys. **125**, 084501 (2006).

[36] S. Mukamel, *Principles of Nonlinear Optical Spectroscopy* (Oxford University Press, New York, Oxford, 1995).

[37] W. B. Bosma, Y. J. Yan, and S. Mukamel, Phys. Rev. A **42**, 6920 (1990); Y. J. Yan and S. Mukamel, J. Chem. Phys. **94**, 179 (1991); M. Cho, J.-Y. Yu, T. Joo, Y. Nagasawa, S. A. Passino, and G. R. Fleming, J. Phys. Chem. **100**, 11944 (1996); G. R. Fleming and M. H. Cho, Annu. Rev. Phys. Chem. **47**, 109 (1996).

[38] R. Jimenez, G. Salazar, J. Yin, T. Joo, and F. E. Romesberg, Proc. Natl. Acad. Sci. U.S.A. **101**, 3803 (2004).

[39] M. H. Vos, J. C. Lambry, S. J. Robles, D. C. Youvan, J. Breton, and J. L. Martin, Proc. Natl. Acad. Sci. U.S.A. **88**, 8885 (1991); M. H. Vos, F. Rappaport, J. C. Lambry, J. Breton, and J. L. Martin, Nature (London) **363**, 320 (1993); K. R. Shelly, E. A. Carson, and W. F. Beck, J. Am. Chem. Soc. **125**, 11810 (2003).

[40] As reported by the Mathies group, the spectral width of the transient Raman spectrum of β-carotene is about 70 cm^{-1} at maximum (Ref. 41), which indicates that the dephasing time in the excited states is longer than 150 fs. Since the decay time from S_2 is S_x is much faster than this time constant, the S_2 to S_x cannot reflect the dephasing process in the S_2 state and so S_x should be an electronic level. For more details, see Ref. 16.

[41] P. Kukura, D. W. McCamant, and R. A. Mathies, J. Phys. Chem. A **108**, 5921 (2004).

[42] Q. H. Xu, G. D. Scholes, M. Yang, and G. R. Fleming, J. Phys. Chem. A **103**, 10348 (1999); M. Yang, K. Ohta, and G. R. Fleming, J. Chem. Phys. **110**, 10243 (1999); Q. H. Xu and G. R. Fleming, J. Phys. Chem. A **105**, 10187 (2001); R. Jimenez and F. E. Romesberg, J. Phys. Chem. B **106**, 9172 (2002); J. Stenger, D. Madsen, P. Hamm, E. T. J. Nibbering, and T. Elsaesser, J. Phys. Chem. A **106**, 2341 (2002); Q. H. Xu, Y. Z. Ma, and G. R. Fleming, *ibid.* **106**, 10755 (2002); E. T. J. Nibbering and T. Elsaesser, Chem. Rev. **104**, 1887 (2004).

[43] The allowance to obtain a good agreement between the experiment and calculation is about 2 cm^{-1}.

[44] F. S. Rondonuwu, Y. Watanabe, R. Fujii, and Y. Koyama, Chem. Phys. Lett. **376**, 292 (2003).

[45] S. Mukamel, A. E. Cohen, and U. Harbola, in *Time-Dependent Density Functional Theory*, Lecture Notes in Physics, edited by M. A. L. Marques, C. A. Ullrich, F. Nogueira, A. Rubio, K. Burke, and E. K. U. Gross (Springer-Verlag, Berlin, 2006), p. 107.

[46] We have also calculated the TG signals assuming only the S_2 and S_1 states, namely, S_x is eliminated. However, a good agreement was not attained (result is not shown).

[47] The decay times shown in Fig. 5 are slightly faster than the vibronic decoherence times obtained by the calculations. This is because the decay times in Fig. 5 reflect both the electronic and vibronic decays.

[48] A. N. Macpherson, J. B. Arellano, N. J. Fraser, R. J. Cogdell, and T. Gillbro, Biophys. J. **80**, 923 (2001).

[49] The branching ratio between $S_1 \rightarrow S_0$ and $S_1 \rightarrow Q_y$ can be obtained from the percentage composition of the internal-conversion rates, i.e., $\Gamma_{10}:\Gamma_{1Q_y}=22\%:78\%$, which is very close to the results obtained in the previous reports (Refs. 5–7 and 24–27). Since these pathways have an error of ± 0.5 ps, the branching ratio varies $\pm 5\%$. The efficiency of the excitation energy transfer is then given by the product of the inflow from the upper singlet state S_x and the percentage composition of the $S_1 \rightarrow S_0$ pathway. Therefore, the efficiency significantly depends on the lifetime of the upper singlet state.